

*Original Research*

# Transplanted OECs Protect Visual Function by Regulating the Glutamate Metabolic Microenvironment in the Glaucoma Model

Hui Gao<sup>1,2</sup>, Siyu Chen<sup>1,2</sup>, Luodan A<sup>1,2</sup>, Haiwei Xu<sup>1,2</sup>, Jing Xie<sup>1,2,\*</sup>, Zheng Qin Yin<sup>1,2,\*</sup><sup>1</sup>Southwest Hospital/Southwest Eye Hospital, Third Military Medical University (Army Medical University), 400038 Chongqing, China<sup>2</sup>Key Lab of Visual Damage, Regeneration and Restoration of Chongqing, 400038 Chongqing, China\*Correspondence: [xiejingrain@163.com](mailto:xiejingrain@163.com) (Jing Xie); [qinzyin@aliyun.com](mailto:qinzyin@aliyun.com) (Zheng Qin Yin)

Academic Editor: Gernot Riedel

Submitted: 19 October 2022 Revised: 9 November 2022 Accepted: 14 November 2022 Published: 6 May 2023

## Abstract

**Background:** Glaucoma is the leading cause of irreversible blindness, and the loss of retinal ganglion cells (RGCs) is the most important pathological feature. During the progression of glaucoma, glutamate content in the optic nerve increases, and glutamate-induced excitotoxicity will aggregate the damage and death of RGCs. We have previously reported that olfactory ensheathing cells (OECs) transplantation preserved the visual function of the glaucoma model but the mechanism is unknown. **Methods:** Adult Long-Evans rats were used in the present study and injecting magnetic microspheres was used to establish a glaucoma model in rats. Optokinetic response test and Pattern electroretinogram recording were used to assess the visual functions of rats. RT-PCR, immunofluorescence, and co-culture experiments were performed to investigate the therapeutic effects and mechanisms of OECs for glaucoma. **Results:** In the glaucoma model, increased glutamate content and the damage of astrocytes (AC) and RGCs were observed. OECs transplantation reduced the glutamate concentration in the optic nerve, alleviated the apoptosis of AC and RGCs, and protected the visual function of the glaucoma model. Furthermore, we found that OECs possessed a stronger capacity to metabolize excessive glutamate compared with AC and Müller glia. OECs could improve the glutamate microenvironment of the optic nerve to prevent AC and RGCs from glutamate-induced excitotoxicity in glaucoma. And the recovery of AC function further supported the survival of RGCs. **Conclusions:** We demonstrate that OECs transplantation could play a neuroprotective role by regulating the glutamate microenvironment in glaucoma.

**Keywords:** glaucoma; OECs; astrocyte; glutamate metabolism

## 1. Introduction

As the most common cause of global irreversible blindness, glaucoma is a group of heterogeneous diseases characterized by progressive optic nerve damage and retinal ganglion cells (RGCs) death, leading to permanent visual field loss and blindness eventually [1]. Worldwide, the prevalence of glaucoma for people aged 40–80 is 3.5%, and an estimated 70 million people have glaucoma so far [2]. The death of RGCs, the retina's output neurons that convey visual information to the brain, is the most critical pathological event during glaucoma. So figuring out the mechanisms of RGC's death and rescuing RGCs are the key points for glaucoma treatment [3].

The pathogenesis of glaucoma is multifactorial including elevated intraocular pressure (IOP), increased age, vascular dysfunction, and genetic deficit [4]. Recently, multiple intrinsic and extrinsic molecules and signaling pathways were proven to trigger optic nerve axon injury and RGCs apoptosis [3,5]. Among these mechanisms, the neurotoxicity due to the overactivation of N-methyl-D-aspartate (NMDA) receptors by glutamate is regarded as one of the imperative causes of RGCs death [6,7]. Meanwhile, glutamate excitotoxicity will cause astrocyte dysfunction and damage [8]. Astrocytes provide structural, energetic, and trophic support for RGCs by enveloping optic nerve ax-

ons without myelin sheath, participating in optic nerve metabolism, and secreting trophic factors [9]. Meanwhile, astrocytes are the predominant glia participating in glutamate metabolism in the optic nerve and the dysfunction of astrocytes will further elevate the level of glutamate and aggravate the degeneration of axons and RGCs [10]. Therefore, targeting glutamate neurotoxicity and enhancing the supportive functions of astrocytes may be promising strategies for glaucoma treatment.

Olfactory ensheathing cells (OECs), a unique macroglia isolated from the olfactory bulb and the olfactory nerve originated from the embryonic ectoderm of olfactory placodes [11]. OECs that were present in Peripheral Nervous System (PNS) and Central Nervous System (CNS) shared the functional characteristic with astrocytes and Schwann cells and possessed more advantages over them like migration, immunomodulatory and pro-regeneration [11,12]. OECs were first used to treat spinal cord injury and displayed excellent therapeutic potential and the capacity to promote regeneration [13]. Transplanted OECs could envelop injured axons, degrade inhibitory extracellular matrix, modulate the immune response, and secrete neurotrophic factors for CNS repair, leading to extensive nerve regeneration and functional recovery [14]. In previous research, we demonstrated that



OECs transplantation into sub-retinal space could retard retinal degeneration by clearing cell debris, reducing the gliotic response of Müller cells, and regulating the activation of microglia [15–17]. In addition, transplanted OECs were observed to incorporate into the optic papilla where OECs enveloped optic nerve axon in a non-myelination manner, leading to the optic nerve axon regeneration and functional recovery in the optic nerve injury model [18,19]. The interaction between OECs and astrocytes could regulate the astrocyte reactivity, alleviate neurotoxicity, rearrange glial scar, and format “a bridge” that permits axon regeneration, which was recognized as the vital mechanism for CNS repair [20–22]. Considering the regulatory effect of OECs on astrocytes, glutamate excitotoxicity, and astrocyte functions in the optic nerve, we think OECs may involve in the regulation of glutamate metabolism and astrocyte function in glaucoma. But the relationship between glutamate metabolism, astrocyte function, and RGCs injury in glaucoma after OECs transplantation was unknown.

In the present research, we established an elevated IOP glaucoma rat model in which visual function declined progressively, accompanied by optic nerve fiber damage and astrocyte gliosis by injecting magnetic microspheres into the anterior chamber. The transplantation of OECs alleviated optic nerve axon degeneration and astrocyte gliosis, which caused the improvement of visual functions without decreasing IOP. And this protective effect on the optic nerve and visual function last at least 6 weeks. By exploring mechanisms further, we found that OECs possessed a stronger capacity to metabolize glutamate than astrocytes and Müller glia by expressing high-level glutamate metabolism-related enzymes. OECs could decrease glutamate concentration, which contributed to reducing glutamate-induced neurotoxicity for RGCs. On the other hand, OECs also improved glutamate-induced dysfunction and damage of astrocytes, and the supportive functional improvement of astrocytes further promotes the survival of RGCs. In summary, we demonstrated that OECs transplantation is a prospective treatment for glaucoma.

## 2. Materials and Methods

### 2.1 Animal and the Establishment of the Glaucoma Model

Adult Long-Evans (LE) rats regardless of sex used in this study were provided by the Animal Centre of the Third Military Medical University (Army Medical University). Rats were maintained in the Animal Center of Southwest Hospital under a regular 12 h light/dark cycle. LE rats were worn animal masks and anesthetized by inhalation mixed O<sub>2</sub> and isoflurane. Oxybuprocaine hydrochloride eye drops were used for ocular surface anesthesia. 20  $\mu$ L of 30 mg/mL magnetic microspheres suspension was injected into the anterior chamber from the corneal limbus with a 33 G needle. After injection, magnetic microspheres were distributed at the angle of the anterior chamber by a

small magnet to block the trabecular meshwork [23].

### 2.2 The Measure of IOP

IOP of all rats was measured in both eyes 1 day before and 1 day after microspheres injection, then weekly until 8 weeks post-injection (wpi) in a dark room from 9:00 AM to 10:00 AM. After rats were anesthetized by inhalation successfully, the Icare tonometer was used to quickly measure IOP in both eyes of glaucoma rats three times, and the average value was taken.

### 2.3 Solation and Purification of OECs

OECs were isolated and purified from nerve layers of olfactory bulbs from adult LE rats as described previously [16]. After being anesthetized deeply with pentobarbital sodium (10 mg/kg; Sigma-Aldrich, St. Louis, MO, USA). The nerve layer was isolated from the olfactory bulb, cut into 0.5 mm<sup>3</sup> small pieces, and digested for 15 min with 0.1% trypsin (Gibco, Grand Island, NY, USA) under 37 °C and 5% CO<sub>2</sub>. Primary OECs were cultured in DMEM/F12 with 10% Fetal Bovine Serum (FBS) and 1% PS for 5 days and then changed culture medium every 3 days. When OECs reached 80%–90% confluence, the Nash differential adhesion method is used to purify OECs. Then, OECs that were purified 2–3 times were identified and used for sub-retinal transplantation and co-culture experiment.

### 2.4 Subretinal Transplantation

OECs were digested into single-cell suspension in Phosphate-Buffered Saline (PBS) for transplantation, as previously described [15]. Rats were anesthetized by intramuscular injection of sodium pentobarbital (10 mg/kg). Oxybuprocaine hydrochloride eye drops were used for ocular surface anesthesia, and compound tropicamide was used for mydriasis. The bulbar conjunctiva of the corneoscleral limbus was cut with microscissors, and the bulbar conjunctiva and fascia were bluntly separated to expose the sclera. Anterior chamber puncture was performed at the limbus to flow out aqueous humor. The sclera was punctured at 2 mm behind the corneoscleral limbus; 10<sup>5</sup> cells/3  $\mu$ L of cell suspension was injected into subretinal space by a 33-gauge Hamilton needle. The right eyes of glaucoma rats were injected into OECs and the left eyes were injected into 3  $\mu$ L PBS.

### 2.5 Optokinetic Response Test

Rats were dark-adapted for 2 hours and then placed on the experimental platform for 1 min before the experiment [24]. The optokinetic test device consisted of upper and lower mirrors, four surrounding computer screens, and a platform located in the center. A camera suspended on the top of the test device was used for recording the behaviors of rats during the test. During the test, a total of 8 bars with different spatial frequency (0.05, 0.075, 0.1, 0.2, 0.3, 0.4, 0.5, and 0.6 cycles/degree from wide to narrow under

100% contrast were applied for detecting the visual acuity. Statistical analysis was performed after the highest spatial frequency with which rats could respond was converted into the corresponding visual acuity.

### 2.6 Pattern Electroretinogram Recording

Pattern electroretinogram (PERG) was recorded as described previously [25]. Rats were dark-adapted over 8 hours and preparations were performed under dim red light before PERG recording. Rats were anesthetized by intramuscular injection of sodium pentobarbital (10 mg/kg) and placed on a heating plate to maintain the body temperature of rats at 37 °C to prevent hypothermia. Briefly, the ring recording electrode made of gold was put on the center of the cornea, the ground electrode was inserted subcutaneously in the tail, and the reference electrode was inserted into the scleral conjunctiva around the equator of the eyes. The generation, amplification of stimulus (0.1–500 Hz band-pass), and data acquisition were performed with a RETIscan system (Roland Consult, Brandenburg, Germany). White and black alternating reversing bars (contrast, 100%; mean luminance, 50 cd/m<sup>2</sup>; spatial frequency, 0.033 cycles per degree; temporal frequency, 1 Hz) were used to generate the stimulus. At a distance of 11 cm from the screen, the projection of the pupil and visual axis were aligned. The average of superimposed 250 sweeps was recorded as a PERG reading. Measurements were made between a peak and adjacent trough of the waveform for the PERG amplitudes.

### 2.7 Tissue Preparation

For cultured cells, cell climbing slices were fixed in 4% paraformaldehyde (PFA) for 15 min. for retinal tissues, after anesthesia with an intramuscular injection of sodium pentobarbital (10 mg/kg), the rats were perfused with 0.9% normal saline through the left ventricle continuously. After the blood was washed out, rats were perfused with 4% PFA solution for internal fixation. Cut the bulbar conjunctiva around the corneal limbus, separated fascia and muscle, and the optic nerve was cut near the orbital apex. The cornea, iris, lens, and vitreous body were cut off, and only the 0.5 mm sclera and optic nerve close to the optic disc were kept. The optic nerve was placed in 4% PFA, fixed at 4 °C for 0.5 hours, gradient dehydrated in 10%, 20%, and 30% sucrose/PB solution, and then put into 30% sucrose/PB solution overnight. Then, the sucrose solution was exhausted, and the optic nerve was embedded in the optimum cutting temperature compound and quickly frozen in liquid nitrogen. A cold microtome was used to cut the tissues into 10- $\mu$ m-thick sections.

### 2.8 Immunofluorescence Staining

Frozen sections were washed three times in PBS, permeabilized with 0.3% Triton X-100 for 10 min, and blocked by 1% goat serum for 1 hour at 37 °C. Frozen sections were

incubated with primary antibody at 4 °C overnight. After washing in PBS three times, sections were incubated in secondary antibody at 37 °C for 30 min. After staining of DAPI, the sections were scanned and photographed by confocal microscopy (Zeiss LSM 880, Oberkochen, Germany). The antibodies and dilutions were used in present study: mouse anti-Tuj1 (ab78078 1:200, Abcam, Cambridge, UK), Rabbit anti-GFAP (ab7260 1:200, Abcam, Cambridge, UK), Rabbit anti-EAAT2 (ab41621 1:200, Abcam, Cambridge, UK), Rabbit anti-GS (ab64613 1:100, Abcam, Cambridge, UK), mouse anti-CRALBP (ab15051 1:50, Abcam, Cambridge, UK), mouse anti-Caspase-3 (ab13847 1:100, Abcam, Cambridge, UK).

### 2.9 Primary Culture and Identification of Astrocytes

Muscle and connective tissue around the eyeball were isolated and removed to expose the optic nerve. The optic nerve was minced and digested in 0.25% trypsin at 37 °C for 40 min, and D/F12 containing 15% FBS and 1% PS was used to terminate digestion. The cell suspension was centrifuged for 5 min, seeded in T75, and cultured at 37 °C. Once cells reached confluence, T75 was shaken on a shaker at 250 rpm for 18 h, the supernatant was removed and fresh medium was added to T75.

### 2.10 Establishment of Glutamate-Induced AC Apoptosis Model

P4 AC (astrocytes) was seeded on a cell climbing slice that was placed in a 24-well plate at 10<sup>5</sup> cells/well. AC was treated with 50 mM, 100 mM, and 200 mM glutamate for 6 and 24 hours to observe the states of the cells.

### 2.11 Primary Culture and Identification of Müller Glia

The eyeball of LE rats at postnatal 8 days was taken out and incubated in dulbecco's modified eagle medium (DMEM) without serum at 4 °C overnight. Then, the retina was separated from the eyeball that was digested in 1 mg/mL trypsin 1 mg/mL type IV collagenase at 37 °C for 40 min, then was mechanically dissociated into a single cell and cultured in DMEM containing 10% FBS for 7 days. Upon reaching complete confluence, Müller glia was trypsinized for purification and identification.

### 2.12 Co-Culture of AC with OECs

P4 AC was cultured in 24-well plates at a density of 1 × 10<sup>5</sup> cells/well and was co-cultured with OECs or AC. OECs were seeded in the transwell chambers at a density of 1 × 10<sup>5</sup>/well in the experimental group and AC were seeded in the transwell chambers at the same density in the control group. Then, cells were cultured in a medium containing 200 mM glutamate for 24 hours for photographing and immunofluorescence staining.

**Table 1. Primers for RT-PCR.**

Genes	Forward primer	Reverse primer
<i>Neurofilament</i>	CACCGACCGCCACCAT	CACGTAGCGCCGCTTGT
<i>GFAP</i>	TCCTGGAACAGCAAACAAG	CAGCCTCAGGTTGGTTCAT
<i>GAPDH</i>	AAGGTCGGTGTGAACGGATT	TGAACTTGCCGTGGGTAGAG
<i>GS</i>	TCCTGTGGCCATGTTTCGAG	GCGGGCTCCGGTTATACTTG
<i>Caspase-3</i>	TACCCTGAAATGGGCTTGTGT	GTTAACACGAGTGAGGATGTG
<i>Bcl-2</i>	CGCCCGCTGTGCACCGAGA	CACAATCCTCCCCAGTTCACC
<i>Bax</i>	GGCGATGAACTGGACAACAA	CCCAGTTGAAGTTGCCGTCT
<i>EAAT1</i>	TCTTGGTTTCGCTGTCTGCCACG	TCCTCATTCATGCCGTTCATCGTCC
<i>EAAT2</i>	ATGTCTTCGTGCATTCCGGTGTGGG	AGCCGTGGCACCATCTTCATAGC
<i>EAAT3</i>	GGGACAGATTCTGGTGGATT	GTGATCCTCTTGTCAC

GFAP, glial fibrillary acidic protein; GAPDH, glyceraldehyde-3-phosphate dehydrogenase; GS, Glutamine synthetase; EAAT1, Excitatory Amino Acid Transporter 1; EAAT2, Excitatory Amino Acid Transporter 2; EAAT3, Excitatory Amino Acid Transporter 3.

### 2.13 Measurement of Glutamate Concentration

Glutamate concentration was measured by a Glutamate detection kit (ab83389, Abcam, Cambridge, UK). Briefly, 0, 2, 4, 6, 8, and 10  $\mu\text{L}$  glutamate solution (1 mM) were added to a 96-well plate and were made up to 50  $\mu\text{L}$  to make a standard curve. 50  $\mu\text{L}$  cell culture supernatant was added to a 96-well plate, then a mixture containing 90  $\mu\text{L}$  buffer, 8  $\mu\text{L}$  chromogenic reagent, and 2  $\mu\text{L}$  glutamate enzyme was added to the 96-well plate. OD value measured by spectrophotometer at 450 nm wavelength after incubating for 30 min at 37 °C was used to Calculate the glutamate concentration according to the standard curve.

### 2.14 Real-Time Quantitative PCR (RT-qPCR)

Total RNAs of cell and optic nerve tissue cells were extracted using RNAiso Plus (Cat. No. D9108A, Takara, Kyoto, Japan). RNA samples were reversed as cDNA by PrimeScript™ RT reagent kit (Cat. No. #RR037A, Takara, Kyoto, Japan). RT-qPCR was used to measure the expression of various genes as previously described [13]. And the expressions were normalized to the level of GAPDH. All primers were listed in Table 1.

### 2.15 Statistical Analysis

All data were analyzed statistically by using SPSS 13.0 (IBM Corp., Chicago, IL, USA). A *T*-test was used to compare the means of two groups and one-way or two-way analysis of variance (ANOVA) was used to compare means among multiple groups. Results are presented in the form of mean  $\pm$  standard deviation ( $\bar{x} \pm s$ ). *p* values < 0.05 were considered to be statistically significant.

## 3. Results

### 3.1 Establishment of the Glaucoma Model

We established the elevated IOP glaucoma model by injecting magnetic microspheres into the anterior chamber of LE rats. Magnetic microspheres were evenly distributed

in the corner of the chamber under the attraction of the magnet, destroying the normal function of the trabecular meshwork (Fig. 1A). Before injection of microspheres, IOP was measured ( $10.75 \pm 0.96$  mmHg). Following injection, IOP raised continuously and reached the peak at 1 week post-injection ( $55.00 \pm 1.41$  mmHg), then fell over gradually and approached a normal level at 7 wpi ( $11.25 \pm 1.89$  mmHg) (Fig. 1B). Then, an optokinetic response test was used to evaluate the visual acuity of normal rats and elevated IOP rats from 2 wpi to 8 wpi (Fig. 1C). The visual acuity gradually declined over time and decreased to  $0.30 \pm 0.07$  c/d at 8 wpi from 0.6 c/d in normal rats (Fig. 1D, *p* < 0.01). Subsequently, the functions of retinal ganglion cells (RGCs) were further assessed by PERG. The amplitudes of P1 and N2 waves declined progressively. The amplitude of the P1 wave measured in normal rats was  $11.42 \pm 2.23$   $\mu\text{V}$ , declined to  $1.38 \pm 0.79$   $\mu\text{V}$  (*p* < 0.01) and the N2 wave amplitude in normal rats was  $14.61 \pm 1.37$   $\mu\text{V}$ , declined to  $1 \pm 0.71$   $\mu\text{V}$  (Fig. 1E–I, *p* < 0.01). Therefore, the injection of magnetic microspheres establishes an elevated IOP glaucoma model in which visual function is damaged.

During intraocular pressure elevation, the structure of neuronal axons stained by Tuj1 gradually was disordered, and the loss of axons was observed in some areas at 2 wpi, and only a small amount of axonal fibers remained at the 8 wpi (Fig. 2A). The gene expression of Neurofilament declined progressively in glaucoma (Fig. 2C, *p* < 0.05). In addition, the changes of astrocytes in the optic nerve region were evaluated by the glial fibrillary acidic protein (GFAP) staining. The optic nerve in normal rats was wrapped by the clear textured GFAP. With the increase of IOP, the structure of GFAP in astrocytes was disorganized and the expression was upregulated, which is most obvious at 4 wpi (*p* < 0.05), and the expression of GFAP decreased slightly at 8 wpi (Fig. 2B,D, *p* < 0.01). These results demonstrate that the nerve fibers of RGCs are lost gradually, accompanied by the gliosis of astrocytes during the pathogenesis of glaucoma.

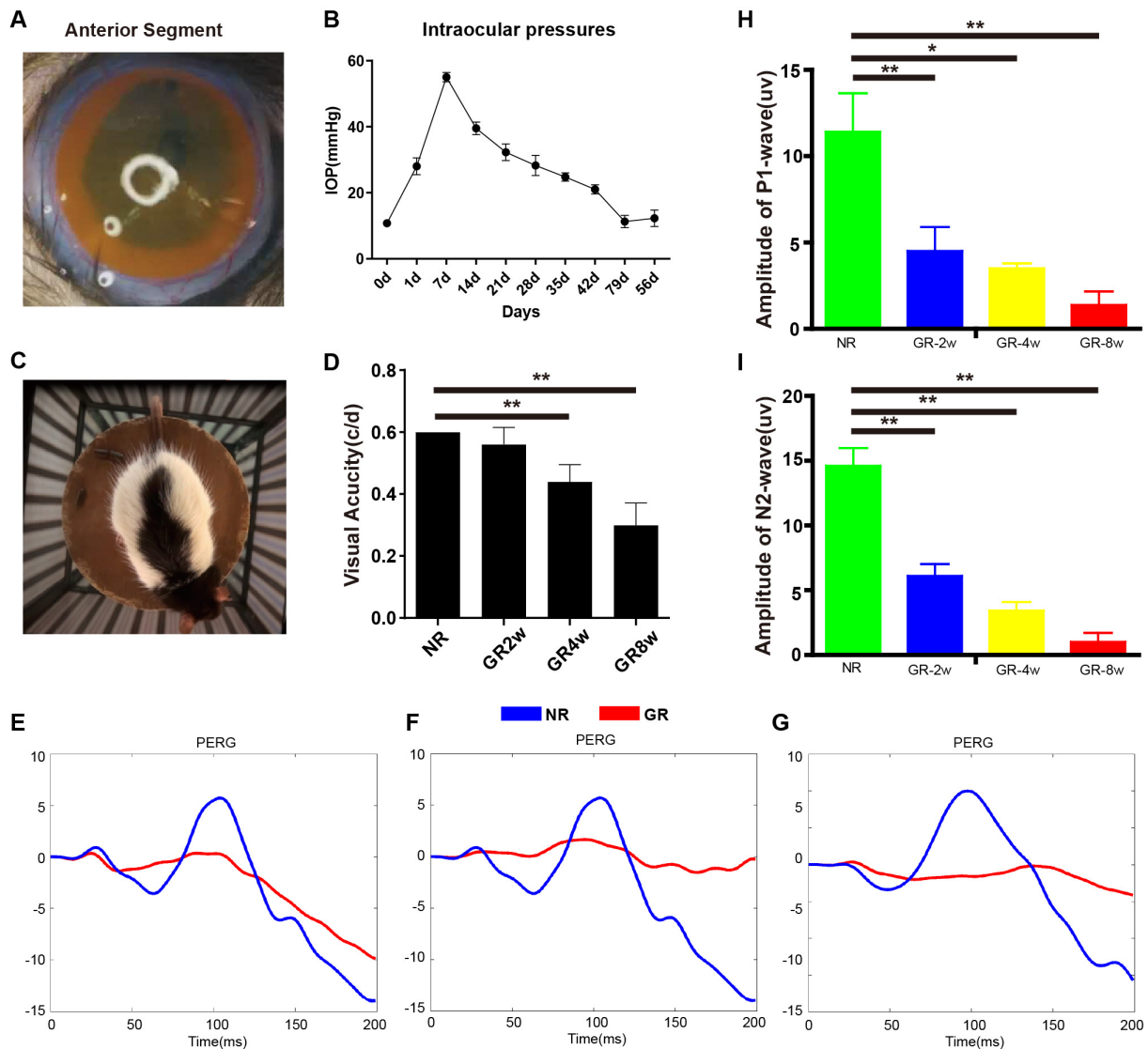


**Fig. 1. The establishment and characteristics of the glaucoma model.** (A) The distribution of magnetic microspheres in glaucoma model rats. (B) Line chart showing the changes of IOP after injection in glaucoma model rats ( $n = 5$ ). (C) Diagram of optokinetic response test. (D) Visual acuity through optokinetic response test from 2 weeks to 8 weeks post-injection ( $n = 5$ ). (E–G) Representative PERG traces in P-wave at 2, 4, and 8 weeks post-injection of magnetic microspheres. (H,I) Diagram showing P1 and N2 wave amplitude in normal and glaucoma model rats ( $n = 4$ ). NR, normal rat; GR, glaucoma rat.  $*p < 0.05$ ,  $**p < 0.01$ . IOP, elevated intraocular pressure; PERG, Pattern electroretinogram.

### 3.2 OECs Transplantation Preserved the Visual Functions and Optic Nerve Structure in Glaucoma

OECs were transplanted into subretinal space 2 weeks after magnetic microspheres injection to rescue the elevated IOP-induced optic nerve injury and PBS was used for control. IOP in OECs and PBS groups declined progressively over time and there was no statistical difference in IOP between the two groups from 1 week post-transplantation (wpt) to 7 wpt (Fig. 3A,  $p > 0.05$ ). The visual acuity of glaucoma model rats increased after OECs transplantation compared PBS group significantly from 2 wpt to 8 wpt (Fig. 3B, 2 w:  $p < 0.01$ ; 4 w:  $p < 0.05$ ; 8 w:  $p < 0.05$ ). Besides, the amplitudes of P1-wave in the OECs group were

higher than in the PBS group at 2 and 6 wpt (Fig. 3C,D, 2 w and 6 w:  $p < 0.05$ ) and this is also the case for N2-wave (Fig. 3C,E, 2 w:  $p < 0.05$ ; 6 w:  $p < 0.01$ ). Tuj1 and GFAP staining was used to further clarify the protective effect of OECs transplantation on the optic nerve of glaucoma model rats. The axon of the optic nerve in the PBS group is lost gradually from the onset of glaucoma and only a few Tuj1<sup>+</sup> regions can be observed at the late stage. In the OECs group, the most of axon was integral and clear at 2 wpt and the area of the Tuj1<sup>+</sup> region was larger than the PBS group at 6 wpt. Meanwhile, the expression of GFAP was decreased in the OECs group compared with the PBS group (Fig. 3F). Consistent with the results of IF, the mRNA

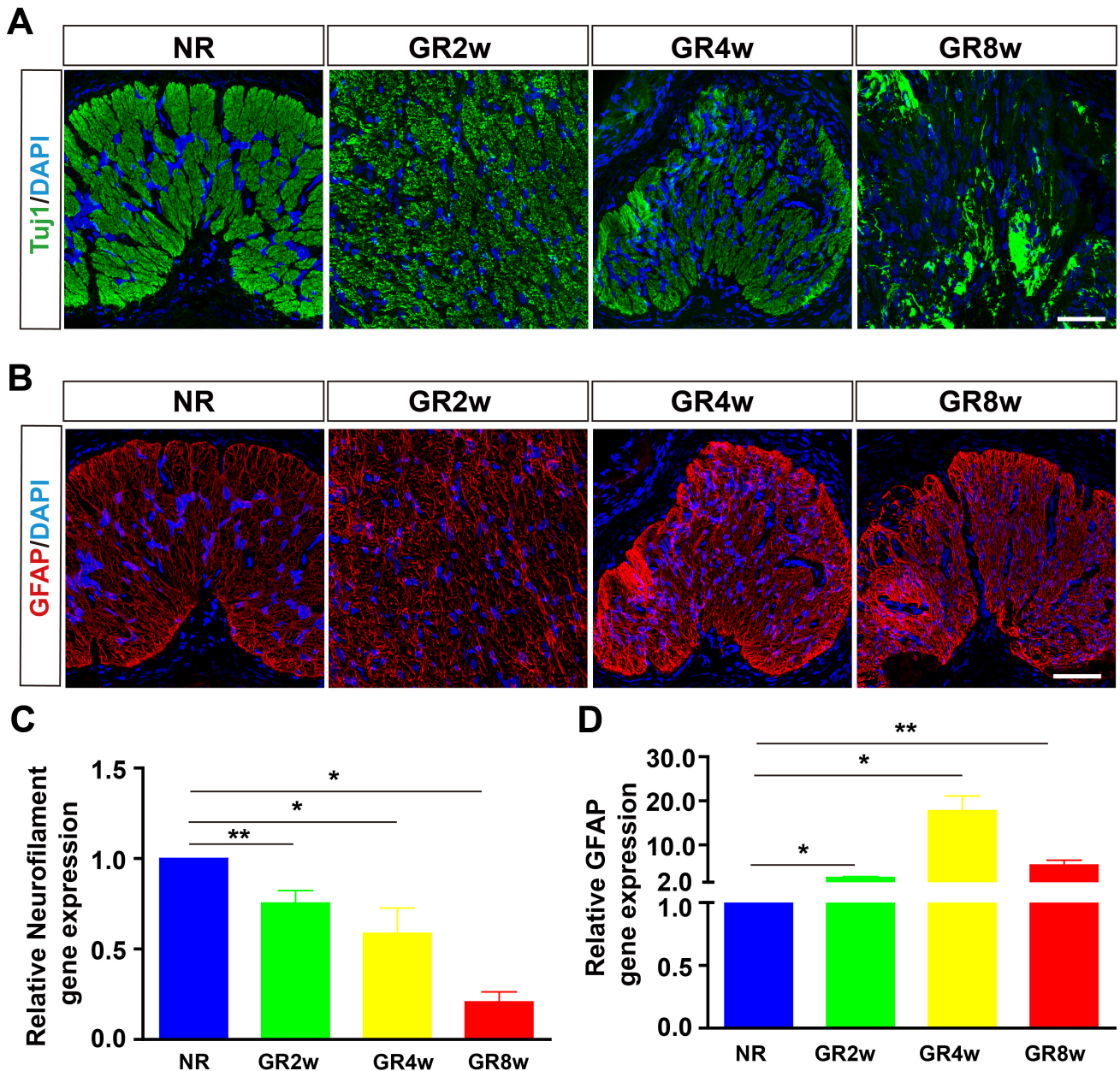


**Fig. 2. Neuronal and glial responses in glaucoma model rats.** (A) Tuj1 staining showing the changes of optic nerve axon in glaucoma model rats. (B) GFAP staining showing the gliosis of astrocytes in glaucoma model rats. (C,D) RT-qPCR analysis showing the relative mRNA expression of Neurofilament and GFAP (n = 9). \* $p < 0.05$ , \*\* $p < 0.01$ . Scale bars: 50  $\mu\text{m}$ .

level of Neurofilament increased in OECs from 2 wpt to 6 wpt (2 w:  $p < 0.05$ ; 4 w:  $p < 0.05$ ; 6 w:  $p < 0.01$ ) and GFAP mRNA level in OECs was lower than PBS group (4 w:  $p < 0.05$ ; 6 w:  $p < 0.05$ ) (Fig. 3G,H). Thus, these suggest that OECs transplantation can preserve visual functions of glaucoma model rats, protect the axon of the optic nerve and alleviate the gliosis of astrocytes.

### 3.3 OECs Reduced Glutamate-Induced AC Apoptosis *in Vitro*

Due to the key role of glutamate in the pathogenesis of glaucoma and the fact that AC are important regulators

of glutamate metabolism, we studied the effects of OECs on astrocytes *in vitro*. Firstly, astrocytes isolated from the optic nerve of neonatal rats were identified by glutamine synthetase (GS) staining. P4 astrocytes with large and flat cell bodies had many thick processes, and the positive rate of GS was more than 95% (Fig. 4A). To mimic the glutamate microenvironment of the optic nerve in glaucoma, astrocytes were treated with different concentrations of glutamates. Astrocytes survived well and no apoptosis was observed under 100 mM for 24 h. Under 200 mM glutamate for 6 h, the process of astrocytes retracted, the cell body was atrophied, and apparent apoptosis was observed (Fig. 4B),

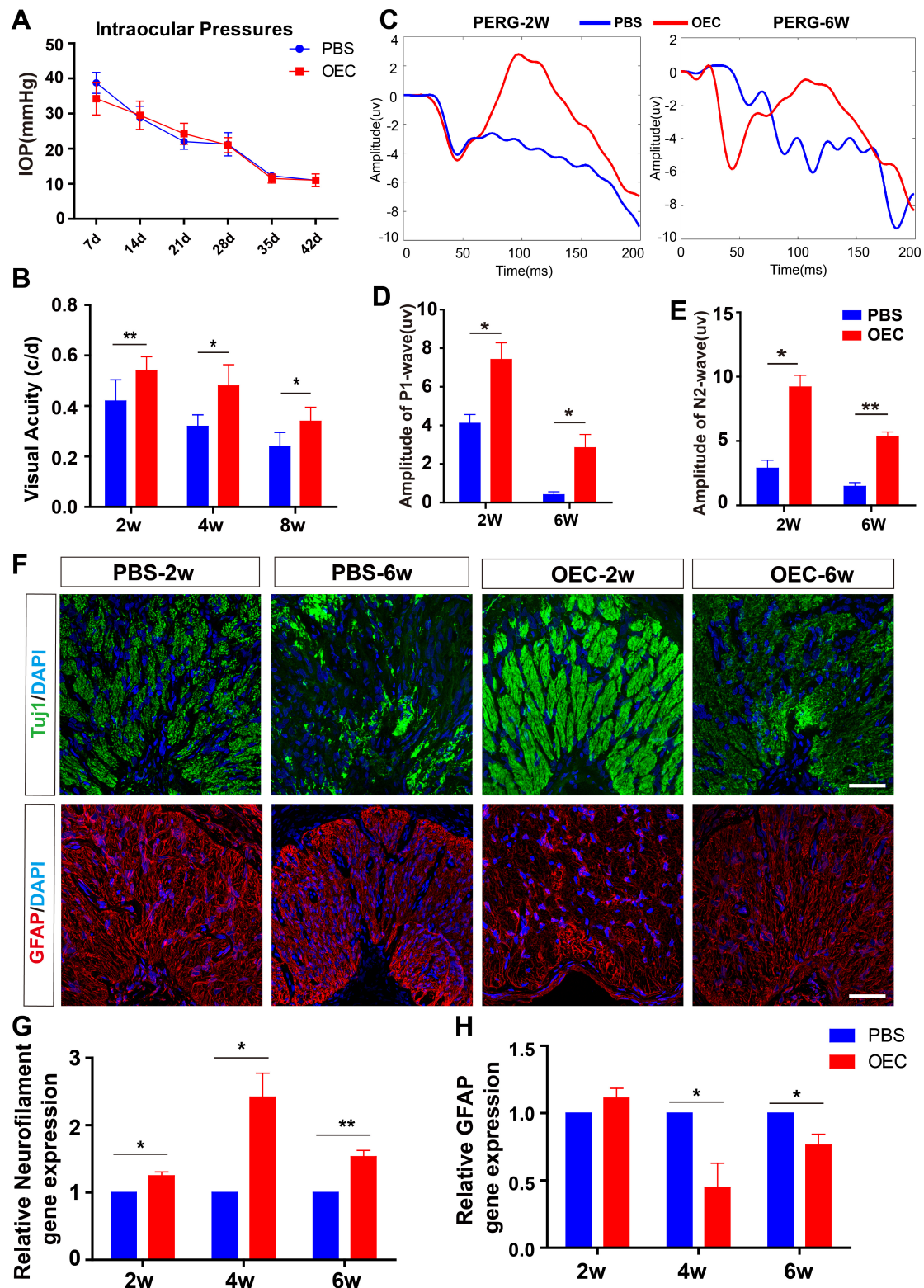


**Fig. 3. OECs transplantation improved the visual functions in glaucoma models.** (A) OECs transplantation decreased the IOP ( $n = 5$ ). (B) Optokinetic response test showing OECs improved visual acuity from 2 weeks to 8 weeks post-transplantation ( $n = 5$ ). (C) Representative PERG traces in P1-wave of the PBS and OECs groups at 2 and 6 weeks post-transplantation. (D,E) OECs improved the amplitudes of P1 and N2 wave in glaucoma model ( $n = 4$ ). (F) Representative images of Tuj1 and GFAP staining in PBS and OECs groups. (G,H) RT-qPCR analysis showing the relative mRNA expression of Neurofilament and GFAP in PBS and OECs groups ( $n = 9$ ).  $*p < 0.05$ ,  $**p < 0.01$ . Scale bars:  $50 \mu\text{m}$ . IOP, elevated intraocular pressure; PERG, Pattern electroretinogram; OECs, olfactory ensheathing cells; PBS, Phosphate-Buffered Saline.

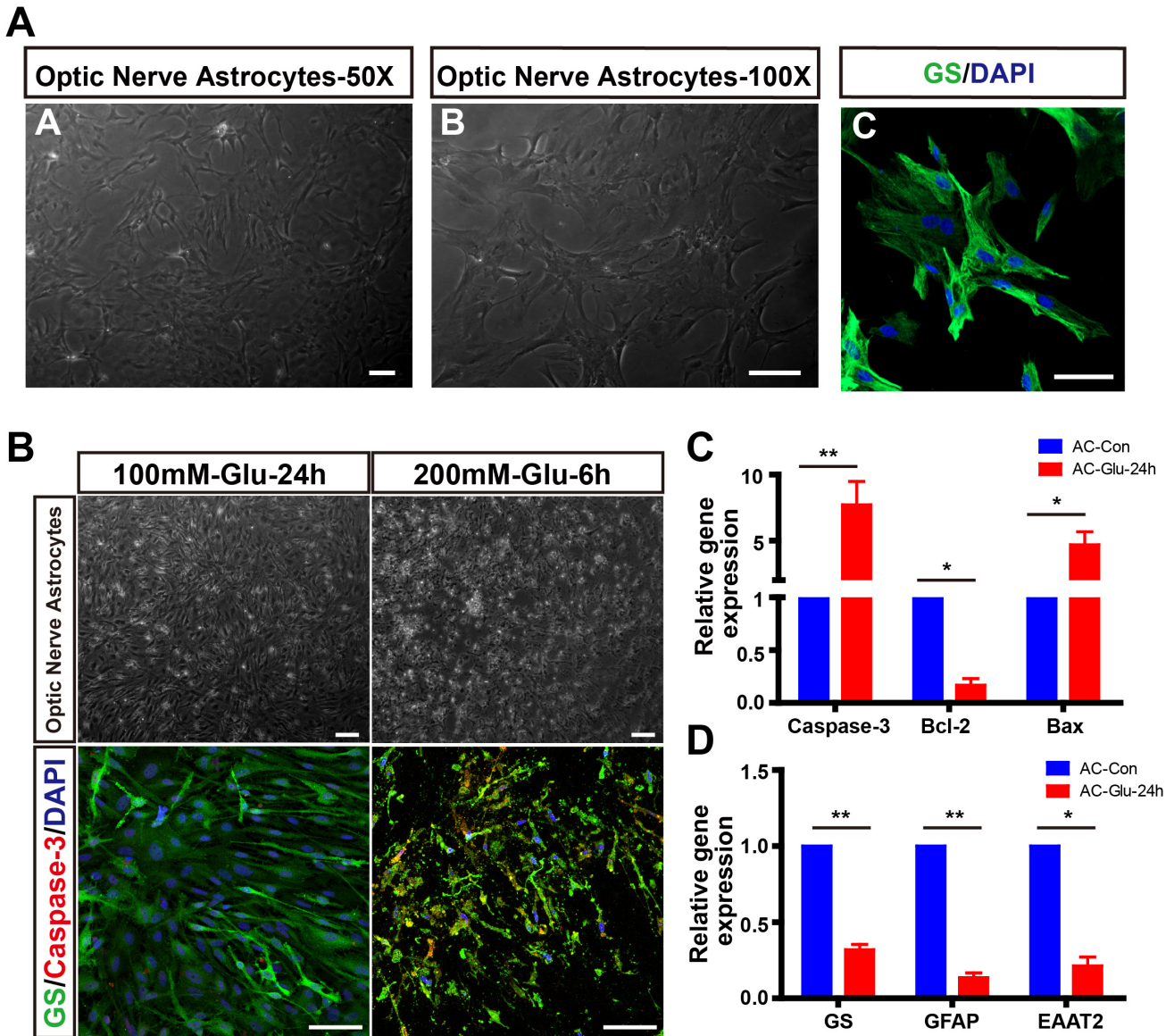


**Fig. 4. Establishment of glutamate-induced astrocytes apoptosis model *in vitro*.** (A) The isolation and identification of primary astrocytes from the optic nerve of neonatal rats. (B) Glutamate induced the apoptosis of astrocytes. (C,D) Relative mRNA expression of GS, GFAP, EAAT2, Caspase-3, Bcl-2, and Bax in normal and glutamate-treated astrocytes for 24 h (n = 3). \* $p < 0.05$ , \*\* $p < 0.01$ . Scale bars: 50  $\mu\text{m}$ .

suggesting that 200 mM glutamate could induce astrocytes apoptosis effectively. Next, RNA was extracted from astrocytes treated with 200 mM for 24 h to detect the changes in gene expression. Apoptosis-related genes Caspase-3 and Bax were upregulated, while apoptosis inhibitory gene Bcl-2 was downregulated (Fig. 4C, Caspase-3:  $p < 0.01$ ; Bcl-2 and Bax:  $p < 0.05$ ). Meanwhile, the gene expression of GFAP and glutamate metabolism related to GS and excitatory amino acid transporter 2 (EAAT2) decreased significantly after astrocytes were treated with 200 mM glutamate (Fig. 4D, GS and GFAP:  $p < 0.01$ ; EAAT2:  $p < 0.05$ ).

Then, co-culturing was used to detect the capacity of OECs to metabolize glutamate and the effects on astrocytes

in the glutamate-induced AC apoptosis model. In the OECs group, the process of astrocytes retracted and cell body size increased, suggesting the activation of astrocytes. However, the morphology of astrocytes was more integral and only a few apoptotic cells were observed compared control group (Fig. 5A). Co-culturing with OECs upregulated the expressions of GFAP, GS, and EAAT2 (Fig. 5D, GS:  $p < 0.05$ ; GFAP and EAAT2:  $p < 0.01$ ). The expression of the anti-apoptosis gene Bcl-2 increased and apoptotic-related genes Caspase-3 and Bax decreased in the OECs group (Fig. 5E,  $p < 0.05$ ). Meanwhile, we found that OECs decreased the glutamate concentration (Fig. 5F,  $p < 0.01$ ). Given that Müller glia was in charge of glutamate

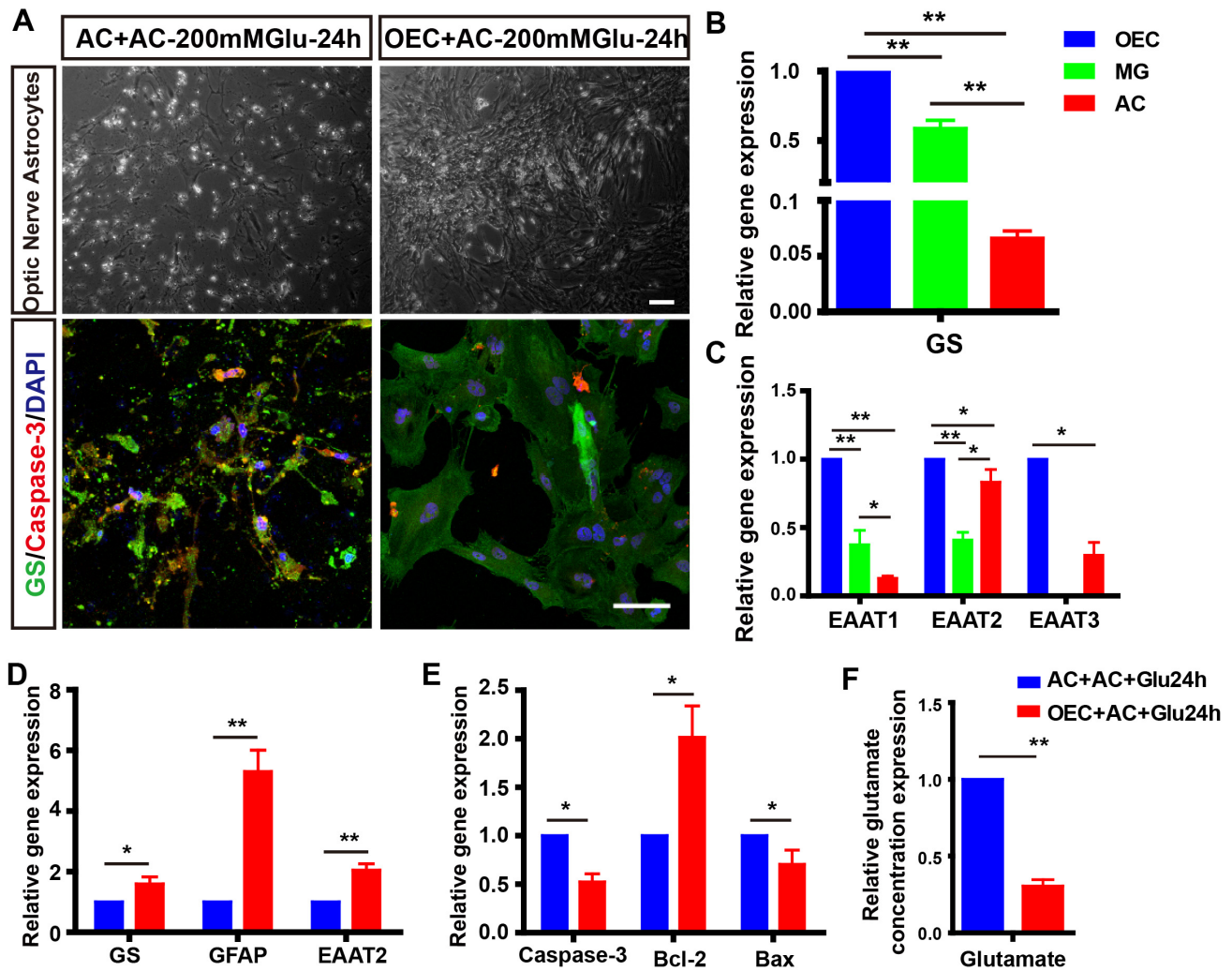


**Fig. 5. Co-culturing with OECs alleviated the glutamate-induced astrocytes apoptosis and dysfunction.** (A) The morphology and Caspase-3 staining of astrocytes co-cultured with/without OECs for 24 h. (B,C) Relative mRNA level of GS, EAAT1, EAAT2, EAAT3 in primary OECs, Müller glia, and astrocytes ( $n = 3$ ). (D,E) Relative mRNA expression of GS, GFAP, EAAT2, Caspase-3, Bcl-2, and Bax in astrocytes co-cultured with/without OECs for 24 h ( $n = 3$ ). (F) Co-culturing with OECs for 24 h decreased relative glutamate concentration in the medium ( $n = 3$ ).  $*p < 0.05$ ,  $**p < 0.01$ . Scale bars: 50  $\mu\text{m}$ . OECs, olfactory ensheathing cells.

metabolism in the retina under normal and glaucoma conditions, we compared the capacity to metabolize glutamate of OECs, Müller glia, and astrocytes. Among three cells, the expression of genes associated with glutamate metabolism in OECs are highest, Müller glia was second and astrocytes were lowest (Fig. 5B,C). In summary, we established a glutamate-induced AC apoptosis model in which AC apoptosis and dysfunction of glutamate metabolism occurred. OECs contributed to reducing AC apoptosis by metabolizing excessive glutamate and maintained the role of glutamate metabolism *in vitro*.

### 3.4 OECs Regulated Glutamate Microenvironment to Rescue Optic Nerve in Glaucoma Model Rats

To explore the effect of OECs transplantation on glutamate metabolism in the optic nerve, we first clarified the

expression of a gene associated with glutamate metabolism in the optic nerve and retina of normal rats. Although GFAP expression in the optic nerve was higher than in the retina, the level of GS and three glutamate transporters EAAT1, EAAT2, and EAAT3 in the optic nerve were lower than retina (Fig. 6A,B, GFAP, GS, EAAT1, and EAAT2:  $p < 0.01$ ; EAAT3:  $p < 0.05$ ), indicating that apoptosis of axons before cell body during glaucoma may be related to the ability of retina and optic nerve to regulate glutamate excitotoxicity. By immunostaining, GS and EAAT2 were reduced significantly from 4 wpi and little GS was observed in the optic nerve at 8 wpi (Fig. 6C,D). Consistent with the results of IF, the gene expressions of GS and EAAT2 declined from 4 wpi to 8 wpi compared to normal rats (Fig. 6E, 4 w:  $p < 0.05$ ; 8 w:  $p < 0.01$ ). Conversely, the relative glutamate concentration increased continuously from 2 wpi to

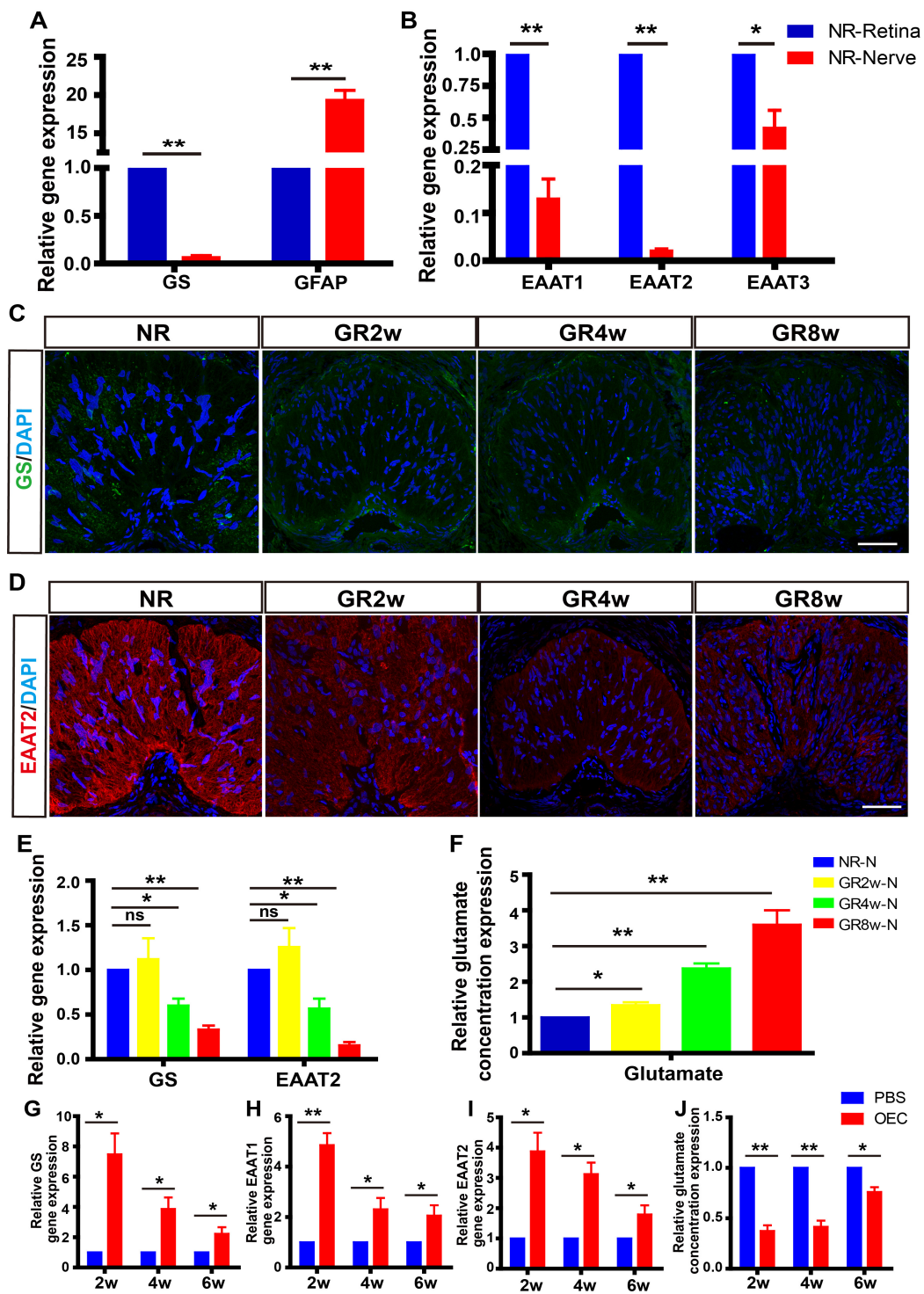


**Fig. 6. Grafted OECs improved the capacity for glutamate metabolism in the glaucoma model.** (A,B) Relative gene expression of GS, EAAT1, EAAT2, EAAT3 in the retina and optic nerve of normal rats (n = 9). (C,D) Representative images of GS and EAAT2 staining in normal and glaucoma model rats at different timepoints. (E) Relative gene expression of GS, EAAT2 in optic nerve of normal and glaucoma model rats at different timepoints (n = 9). (F) Relative glutamate concentration in the optic nerve of normal and glaucoma model rats at different timepoints (n = 9). (G–I) Relative gene expression of GS, EAAT1, EAAT2 in optic nerve of PBS and OECs groups at different timepoints (n = 9). (J) Relative glutamate concentration in the optic nerve of PBS and OECs groups at different timepoints (n = 9). \* $p < 0.05$ , \*\* $p < 0.01$ . Scale bars: 50  $\mu\text{m}$ . OECs, olfactory ensheathing cells; PBS, Phosphate-Buffered Saline.

8 wpi (Fig. 6F, 2 w:  $p < 0.05$ ; 4 w:  $p < 0.01$ ; 8 w:  $p < 0.01$ ). These results show that the functions of AC for glutamate transport and metabolism are reduced and the glutamate content in the optic nerve increase with the progression of glaucoma, which may aggravate the damage of axons.

Following OECs transplantation, the expressions of GS, EAAT1, and EAAT2 in the optic nerve of glaucoma rats increased significantly compared with the PBS group at 2 wpt (GS:  $p < 0.05$ ; EAAT1:  $p < 0.01$ ; EAAT2:  $p < 0.05$ ). The levels of these genes decreased but were higher than that in the PBS group at 4 wpt and 6 wpt (Fig. 6G–I,  $p < 0.05$ ). In addition, OECs reduced the relative glutamate concentration from 2 wpt to 6 wpt (Fig. 6J, 2 w and 4 w:  $p < 0.01$ ; 6 w:  $p < 0.01$ ). Therefore, OECs transplantation contributed to enhancing the functions of glutamate metabolism, improving the glutamate microenvironment in the optic nerve area of glaucoma model rats, reducing RGCs apoptosis caused by excitotoxicity

#### 4. Discussion

OECs Transplantation is a promising treatment for retinal neurodegenerative diseases, especially for axon injuries like glaucoma [26]. The dysfunction of AC and glutamate-induced neurotoxicity were recognized as the vital causative factors during the pathogenesis of glaucoma [8,9]. Here, we reported that OECs transplantation improved the glutamate microenvironment, reduced the glutamate-induced damage of AC and RGCs axons, and significantly preserved the visual function of glaucoma model rats at least 8W. Therefore, OEC transplantation is a potential therapeutic strategy for glaucoma.

Establishing a stable, controllable, and easy-to-operate model is necessary for revealing the pathogenesis mechanisms and seeking therapy for glaucoma. In the field of glaucoma research, rats were widely applied for glaucoma model establishment, due to the similarities in anatomy and aqueous humor system to humans [27]. Moreover, the astrocyte gliosis and dysfunction, axon apoptosis, and RGCs apoptosis were similar to pathological features in humans during glaucoma [28]. Injection of magnetic microspheres to block the trabecular meshwork led to a constant IOP increase, which could simulate elevated IOP glaucoma [23]. In the present study, magnetic microspheres suspension was injected into the anterior chamber of rats to establish glaucoma. IOP increased on the first day after the injection, reached a peak value at 1 wpi, decreased slowly from 2 wpi to 6 wpi, and returned to the normal level at 7 wpi. The damage to the axon and gliotic responses were observed from 2 wpi, and the apoptosis of most axons occurred in the optic nerve at 4 and 8 wpi. It showed that the injection of magnetic microspheres could effectively establish an elevated IOP glaucoma model.

Considering that IOP reached peak value and neural injury was initiated at 1 wpi, then axon injury was observed

at 2 wpi, we transplanted OECs into the subretinal space of glaucoma rats at 2 wpi. First, we used an optokinetic response test to evaluate the visual acuity of glaucoma after OECs transplantation. Results showed the visual acuity at 4 wpi in the OECs group is equivalent to that at 2 wpi in the PBS group, suggesting that OECs transplantation resulted in the increased visual acuity of glaucoma rats during the critical period of optic neuropathy significantly. Then, PERG was used to detect the functional changes of RGCs. P-ERG consisting of P1 and N2 wave mainly originating from retinal ganglion cells was induced by the stimulation of a checkerboard, grid, or other patterns, which was considered the sensitive indicators for glaucoma diagnosis [29]. The amplitudes of P1 and N2 waves declined constantly in glaucoma rats, and OECs transplantation caused the increased amplitudes of P1 and N2 waves compared with the PBS group, indicating that OECs retarded the aggravation of visual function significantly.

Previous research showed that excessive glutamate led to the activation of astrocytes at the early stage and damage of astrocytes characterized by process retracting, and cytoskeleton depolymerization at the late stage [30,31]. The astrocyte damage resulted in the exposure, nutrient deprivation, and apoptosis of optic nerve axons [9]. We found that AC wrapping the axon was well-textured and expressed low levels of GFAP, providing nutritional support for the axon of RGCs. The cell body of AC was gradually hypertrophied and the processes were thickened during the progression of glaucoma. The expression of GFAP increased significantly at 4 wpi and decreased at 8 wpi compared with 4 wpi, which was coincident with previous reports [32]. OECs transplantation alleviated the gliotic reactivity of astrocytes by the staining of GFAP. Coherently, the damage to the optic nerve axon was reduced in the OECs group. Hence, OECs transplantation could protect optic nerve axons and AC in glaucoma rats.

Plenty of clinical and preclinical evidence indicated that glutamate-induced neurotoxicity was of the important causes of axon and RGC damage [7,33]. And regulating glutamate metabolism and suppressing glutamate-induced excitotoxicity contributed to preventing RGC death and retarding the progression of glutamate [6,33,34]. It was reported that axons in the optic disc and lamina cribrosa released glutamate in the form of vesicles and activated glutamate receptors in the glaucoma model [6]. However, with the progression of glaucoma, the ability of activated AC to metabolize glutamate decreased due to the weak ability of glutamate metabolism in the optic nerve, and the local glutamate concentration increased. This caused a series of morphological changes and dysfunction in AC, which in turn led to glial and axonal apoptosis [7,8]. Here, we first treated AC with glutamate to mimic the glutamate-induced AC damage and apoptosis in glaucoma. Following being treated with 200 mM glutamate for 24 h, AC showed, irregular nuclear morphology, a large amount of apoptosis, and

genes associated with glutamate metabolisms like GS and EAAT2 were reduced. However, co-culturing with OECs reversed the glutamate-induced excitotoxicity on AC and reduced the relative glutamate concentration partly. According to reports, the high concentration of extracellular glutamate impeded the transporter function, thereby overactivating glutamate receptors, leading to the large influx of calcium, and eventually causing irreversible cell damage [8,35]. Metabolizing excessive glutamate to reduce glutamate-induced excitotoxicity may be one of the critical mechanisms by which OECs rescued AC. Coherently, we found that OECs possessed the strongest capacity to metabolize glutamate among OECs. Müller glia and AC. Meanwhile, the ability of glutamate metabolism increased, and the glutamate microenvironment was improved in the optic nerve in glaucoma rats after OECs transplantation. Interestingly, OECs were applied for the treatment of lots of neurodegenerative disorders, such as spinal cord injury, stroke, Parkinson's disease that were accompanied by the glutamate-induced excitotoxicity [36,37]. Our results suggested that the regulation of OECs on glutamate metabolism may play an important role in treating these disorders.

In summary, we demonstrated that OECs could improve the glutamate microenvironment to reduce the excitotoxicity of AC and RGCs axons. And the reduced excitotoxicity on AC rescued the dysfunction and apoptosis of AC, which further contributed to the survival of RGCs axons to protect visual function in glaucoma model rats.

## 5. Conclusions

Our results demonstrate that excitotoxicity for RGCs and astrocytes induced by elevated glutamate level is the important pathogenesis of glaucoma. Furthermore, as the pivotal regulator for homeostasis and glutamate metabolism in the optic nerve, the dysfunction of astrocytes will further aggravate the damage to the optic nerve. Account for the outstanding capacity to metabolize glutamate, OECs contribute to the homeostasis of the glutamate microenvironment against the excitotoxicity of glutamate for RGCs. Consequently, OECs transplantation promotes the recovery of visual functions in the glaucoma model. Thus, the strategy of OECs transplantation is promising for glaucoma therapy.

## Availability of Data and Materials

All the data and materials are availability in the main text.

## Author Contributions

HG carried out the data analysis and wrote the manuscript. SC and LA collected and assembled the data. ZQY conceived and designed the study. JX carried out the data analysis, was responsible for the financial support, interpreted the data. HX conceived and designed the study,

carried out the data analysis, interpreted the data, and wrote the final version of the manuscript. All authors contributed to editorial changes in the manuscript. All authors read and approved the final manuscript. All authors have participated sufficiently in the work and agreed to be accountable for all aspects of the work.

## Ethics Approval and Consent to Participate

All experimental procedures were approved by the Ethics Committee of Southwest Hospital, Army Medical University, in compliance with the statement for the use of animals from the Association for Research in Vision and Ophthalmology (AMUWEC2020610).

## Acknowledgment

Not applicable.

## Funding

This study is supported by the National Natural Science Foundation of China (NO. 82000921), Natural Science Foundation of Chongqing (NO. cstc2020jcyj-msxmX0981), and Youth Cultivation Project of Army Medical University (NO. 2019XQN09).

## Conflict of Interest

The authors declare no conflict of interest.

## References

- [1] Stein JD, Khawaja AP, Weizer JS. Glaucoma in Adults—Screening, Diagnosis, and Management: A Review. *JAMA*. 2021; 325: 164–174.
- [2] Tham YC, Li X, Wong TY, Quigley HA, Aung T, Cheng CY. Global prevalence of glaucoma and projections of glaucoma burden through 2040: a systematic review and meta-analysis. *Ophthalmology*. 2014; 121: 2081–2090.
- [3] Almasieh M, Wilson AM, Morquette B, Cueva Vargas JL, Di Polo A. The molecular basis of retinal ganglion cell death in glaucoma. *Progress in Retinal and Eye Research*. 2012; 31: 152–181.
- [4] Di Pierdomenico J, Henderson DCM, Giammaria S, Smith VL, Jamet AJ, Smith CA, *et al.* Age and intraocular pressure in murine experimental glaucoma. *Progress in Retinal and Eye Research*. 2022; 88: 101021.
- [5] Baudouin C, Kolko M, Melik-Parsadaniantz S, Messmer EM. Inflammation in Glaucoma: From the back to the front of the eye, and beyond. *Progress in Retinal and Eye Research*. 2021; 83: 100916.
- [6] Seki M, Lipton SA. Targeting excitotoxic/free radical signaling pathways for therapeutic intervention in glaucoma. *Progress in Brain Research*. 2008; 173: 495–510.
- [7] Namekata K, Kimura A, Kawamura K, Guo X, Harada C, Tanaka K, *et al.* Dock3 attenuates neural cell death due to NMDA neurotoxicity and oxidative stress in a mouse model of normal tension glaucoma. *Cell Death and Differentiation*. 2013; 20: 1250–1256.
- [8] Matute C, Domercq M, Sánchez-Gómez MV. Glutamate-mediated glial injury: mechanisms and clinical importance. *Glia*. 2006; 53: 212–224.
- [9] Shinozaki Y, Koizumi S. Potential roles of astrocytes and Müller

cells in the pathogenesis of glaucoma. *Journal of Pharmacological Sciences*. 2021; 145: 262–267.

- [10] Guttenplan KA, Stafford BK, El-Danaf RN, Adler DI, Münch AE, Weigel MK, *et al.* Neurotoxic Reactive Astrocytes Drive Neuronal Death after Retinal Injury. *Cell Reports*. 2020; 31: 107776.
- [11] Ursavas S, Darici H, Karaoz E. Olfactory ensheathing cells: Unique glial cells promising for treatments of spinal cord injury. *Journal of Neuroscience Research*. 2021; 99: 1579–1597.
- [12] Su Z, He C. Olfactory ensheathing cells: biology in neural development and regeneration. *Progress in Neurobiology*. 2010; 92: 517–532.
- [13] Li Y, Field PM, Raisman G. Repair of adult rat corticospinal tract by transplants of olfactory ensheathing cells. *Science (New York, N.Y.)*. 1997; 277: 2000–2002.
- [14] Gómez RM, Sánchez MY, Portela-Lomba M, Ghotme K, Barreto GE, Sierra J, *et al.* Cell therapy for spinal cord injury with olfactory ensheathing glia cells (OECs). *Glia*. 2018; 66: 1267–1301.
- [15] Xie J, Li Y, Dai J, He Y, Sun D, Dai C, *et al.* Olfactory Ensheathing Cells Grafted Into the Retina of RCS Rats Suppress Inflammation by Down-Regulating the JAK/STAT Pathway. *Frontiers in Cellular Neuroscience*. 2019; 13: 341.
- [16] Xie J, Huo S, Li Y, Dai J, Xu H, Yin ZQ. Olfactory Ensheathing Cells Inhibit Gliosis in Retinal Degeneration by Downregulation of the Müller Cell Notch Signaling Pathway. *Cell Transplantation*. 2017; 26: 967–982.
- [17] Huo SJ, Li YC, Xie J, Li Y, Raisman G, Zeng YX, *et al.* Transplanted olfactory ensheathing cells reduce retinal degeneration in Royal College of Surgeons rats. *Current Eye Research*. 2012; 37: 749–758.
- [18] Li Y, Sauv   Y, Li D, Lund RD, Raisman G. Transplanted olfactory ensheathing cells promote regeneration of cut adult rat optic nerve axons. *The Journal of Neuroscience: the Official Journal of the Society for Neuroscience*. 2003; 23: 7783–7788.
- [19] Dai C, Khaw PT, Yin ZQ, Li D, Raisman G, Li Y. Olfactory Ensheathing Cells Rescue Optic Nerve Fibers in a Rat Glaucoma Model. *Translational Vision Science & Technology*. 2012; 1: 3.
- [20] Li Y, Carlstedt T, Berthold CH, Raisman G. Interaction of transplanted olfactory-ensheathing cells and host astrocytic processes provides a bridge for axons to regenerate across the dorsal root entry zone. *Experimental Neurology*. 2004; 188: 300–308.
- [21] Li Y, Li D, Ibrahim A, Raisman G. Repair involves all three surfaces of the glial cell. *Progress in Brain Research*. 2012; 201: 199–218.
- [22] Saglam A, Calof AL, Wray S. Novel factor in olfactory ensheathing cell-astrocyte crosstalk: Anti-inflammatory protein  $\alpha$ -crystallin B. *Glia*. 2021; 69: 1022–1036.
- [23] Samsel PA, Kisiswa L, Erichsen JT, Cross SD, Morgan JE. A novel method for the induction of experimental glaucoma using magnetic microspheres. *Investigative Ophthalmology & Visual Science*. 2011; 52: 1671–1675.
- [24] Zou T, Gao L, Zeng Y, Li Q, Li Y, Chen S, *et al.* Organoid-derived C-Kit<sup>+</sup>/SSEA4<sup>-</sup> human retinal progenitor cells promote a protective retinal microenvironment during transplantation in rodents. *Nature Communications*. 2019; 10: 1205.
- [25] Dai C, Xie J, Dai J, Li D, Khaw PT, Yin Z, *et al.* Transplantation of cultured olfactory mucosal cells rescues optic nerve axons in a rat glaucoma model. *Brain Research*. 2019; 1714: 45–51.
- [26] Yu Y, Li L, Lin S, Hu J. Update of application of olfactory ensheathing cells and stem cells/exosomes in the treatment of retinal disorders. *Stem Cell Research & Therapy*. 2022; 13: 11.
- [27] Pang IH, Clark AF. Inducible rodent models of glaucoma. *Progress in Retinal and Eye Research*. 2020; 75: 100799.
- [28] Stowell C, Burgoyne CF, Tamm ER, Ethier CR, Lasker/IRRF Initiative on Astrocytes and Glaucomatous Neurodegeneration Participants. Biomechanical aspects of axonal damage in glaucoma: A brief review. *Experimental Eye Research*. 2017; 157: 13–19.
- [29] Salgarello T, Cozzupoli GM, Giudiceandrea A, Fadda A, Placidi G, De Siena E, *et al.* PERG adaptation for detection of retinal ganglion cell dysfunction in glaucoma: a pilot diagnostic accuracy study. *Scientific Reports*. 2021; 11: 22879.
- [30] Ju WK, Kim KY, Noh YH, Hoshijima M, Lukas TJ, Ellisman MH, *et al.* Increased mitochondrial fission and volume density by blocking glutamate excitotoxicity protect glaucomatous optic nerve head astrocytes. *Glia*. 2015; 63: 736–753.
- [31] Maciulaitiene R, Pakuliene G, Kaja S, Pauza DH, Kalesnykas G, Januleviciene I. Glioprotection of Retinal Astrocytes After Intravitreal Administration of Memantine in the Mouse Optic Nerve Crush Model. *Medical Science Monitor: International Medical Journal of Experimental and Clinical Research*. 2017; 23: 1173–1179.
- [32] Chidlow G, Casson R, Sobrado-Calvo P, Vidal-Sanz M, Osborne NN. Measurement of retinal injury in the rat after optic nerve transection: an RT-PCR study. *Molecular Vision*. 2005; 11: 387–396.
- [33] Yanagisawa M, Aida T, Takeda T, Namekata K, Harada T, Shinagawa R, *et al.* Arundic acid attenuates retinal ganglion cell death by increasing glutamate/aspartate transporter expression in a model of normal tension glaucoma. *Cell Death & Disease*. 2015; 6: e1693.
- [34] Faiq MA, Wollstein G, Schuman JS, Chan KC. Cholinergic nervous system and glaucoma: From basic science to clinical applications. *Progress in Retinal and Eye Research*. 2019; 72: 100767.
- [35] Brown GC, Bal-Price A. Inflammatory neurodegeneration mediated by nitric oxide, glutamate, and mitochondria. *Molecular Neurobiology*. 2003; 27: 325–355.
- [36] Reshamwala R, Shah M, St John J, Ekberg J. Survival and Integration of Transplanted Olfactory Ensheathing Cells are Crucial for Spinal Cord Injury Repair: Insights from the Last 10 Years of Animal Model Studies. *Cell Transplantation*. 2019; 28: 132S–159S.
- [37] Iovino L, Tremblay ME, Civiero L. Glutamate-induced excitotoxicity in Parkinson’s disease: The role of glial cells. *Journal of Pharmacological Sciences*. 2020; 144: 151–164.